

## Local density of states from spectroscopic scanning-tunneling-microscope images: Ag(111)

Jiutao Li and Wolf-Dieter Schneider

*Institut de Physique Expérimentale, Université de Lausanne, CH-1015 Lausanne, Switzerland*

Richard Berndt

*2. Physikalisches Institut, RWTH Aachen, D-52056, Aachen, Germany*

(Received 5 June 1997)

Electron scattering from steps on the Ag(111) surface has been studied by scanning tunneling microscopy (STM) and spectroscopic STM images of the differential conductance ( $dI/dV$ ). The amplitudes and positions of maxima of  $dI/dV$  deviate significantly from those of the local density of states (LDOS). These deviations are due to variations of the vertical tip position which exponentially affect the tunneling barrier transmission and, hence,  $dI/dV$ . We show that the LDOS can be recovered from simultaneous topographic and spectroscopic measurements. [S0163-1829(97)03236-0]

A knowledge of the local density of states (LDOS) at solid surfaces is fundamental for an understanding of their local physical and chemical properties. In particular, surface states play a crucial role for the chemical reactivity of some catalytically relevant metals.<sup>1</sup> A measurement of the energy dispersion as a function of the electron wave vector  $E(K)$  of such confined electron states is usually performed by techniques such as angle-resolved photoemission spectroscopy (PES) for occupied states or inverse photoemission spectroscopy for empty states, which are selective in both energy and  $k$  space.<sup>2</sup> Recently, scanning tunneling microscopy (STM) has been used to determine  $E(K)$  from standing waves near steps.<sup>3,4</sup> The STM images can often be interpreted as maps of the sample LDOS  $\rho_s$  near the Fermi energy  $E_F$ .<sup>5</sup> Spectroscopic information on  $\rho_s$  can be extracted from the variation of the tunneling current  $I$  with the sample bias voltage  $V$ . Since  $I$  and hence the constant-current image involve an integral over a range of electron energies its derivative  $dI/dV$  is commonly used to unravel the spectroscopic information, e.g., in spatial maps of  $dI/dV$ . The perhaps most spectacular applications of this spectroscopic measurement have been the direct imaging of superconductor vortices<sup>6</sup> and of electron scattering and confined electronic states on noble metal surfaces.<sup>3,4</sup>  $dI/dV$  mapping is widely used on semiconductor surfaces and interfaces.<sup>7,8</sup>

A caveat commonly mentioned in this context is that  $dI/dV$  is affected, e.g., by local variations of the tip-sample distance  $z$  and therefore does not exactly represent  $\rho_s$ .<sup>3,4,8-10</sup> Strosio *et al.* suggested that this effect can approximately be corrected for by normalization of  $dI/dV$  images with  $I/V$ , a procedure that had proved to be useful for local  $dI/dV$  spectra.<sup>8</sup> Recently, in a theoretical study, Hörmandinger demonstrated that neither maps of  $dI/dV$  nor of the normalized quantity  $(dI/dV)/(I/V)$  are good approximations of the LDOS.<sup>10</sup> Later on Ukrainsev pointed out the decisive role of the barrier transmission probability for recovering the LDOS from  $dI/dV$  spectra.<sup>11</sup> As a consequence, the surface state dispersion evaluated directly from either  $dI/dV$  or  $(dI/dV)/(I/V)$  maps deviates from PES results. Hörmand-

inger suggested that the preferable way for measuring the dispersion was to observe  $dI/dV$  at constant tip height and far away from a step. Unfortunately, at large distances from the step edge, the oscillatory signal becomes smaller. More importantly, while a constant height can be approximated experimentally by constant current operation at a suitable voltage such a voltage is not known *a priori*.<sup>8</sup> Here we use simultaneous measurements of  $z$  and  $dI/dV$  to recover the oscillating LDOS  $\rho_s$  on a close-packed metal surface. Moreover, experimental  $dI/dV$  data are compared to WKB model calculations which take the barrier transmission into account. The agreement of the dispersion thus determined and PES data is very encouraging.

The experiments were performed with a custom-built ultrahigh vacuum (UHV) STM at  $T=50$  K.<sup>12</sup> The Ag(111) surface and  $W$  tips were prepared in UHV by standard procedures.<sup>12</sup> Spectroscopic  $dI/dV$  (using lock-in detection) and constant current images were acquired simultaneously. With modulation amplitudes of 3.5 mV (rms), frequencies of  $\sim 23$  kHz and lock-in time constants of 20 ms, the image data were taken at 80 ms per pixel in order to avoid time-constant effects.

Figure 1 shows cross sections of both a constant current and a  $dI/dV$  image of a monatomic step on Ag(111) at  $V=20$  mV. While a clear oscillatory behavior of  $dI/dV$  with a wavelength of  $32 \text{ \AA}$  is observed the constant current data display a small undulation only with  $\sim 0.1 \text{ \AA}$  corrugation [inset of Fig. 1(a)]. The physical origin of both oscillations has been discussed by Crommie, Lutz, and Eigler<sup>3</sup> and by Hasegawa and Avouris.<sup>4</sup> Scattering of surface state electrons from the step edge leads to interference of the incident and the scattered waves<sup>13</sup> which results in a standing wave pattern in  $\rho_s$ . At low  $V$ , constant current images may be interpreted as maps of  $\rho_s$  (Ref. 5) and thus exhibit oscillations. At larger  $V$  the tunneling current represents a weighted integral over a range of energies.<sup>9</sup> Since these energies correspond to varying wavelengths the oscillatory pattern is washed out in the constant current data.

In a one-dimensional model  $dI/dV$  is given by<sup>9</sup>

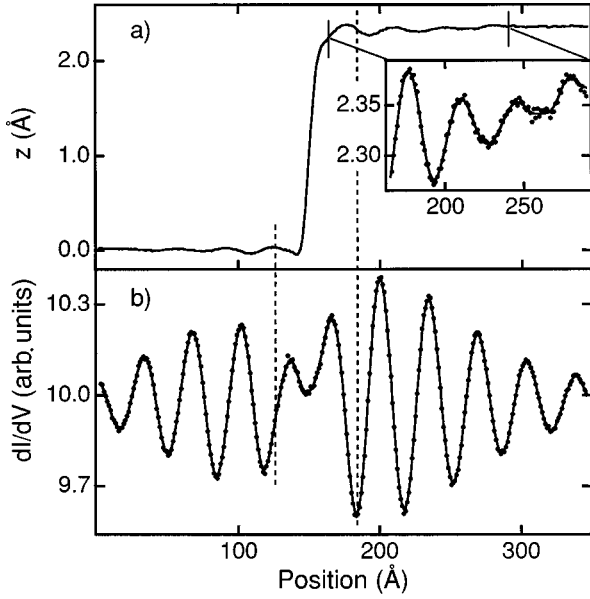


FIG. 1. Cross sections of a constant current (a) and a  $dI/dV$  (b) image of a monatomic step on Ag(111) acquired at  $V=20$  mV and  $I=2.0$  nA. All experimental cross sections are obtained by averaging over 40 line scans. The dashed vertical lines indicate the lateral shift between the features of the two data sets.

$$\frac{dI}{dV} \propto \rho_t(0)\rho_s(eV)T(eV, eV) + \int_0^{eV} \rho_s(E)\rho_t(eV-E) \frac{dT(E, eV)}{dV} dE, \quad (1)$$

where  $\rho_t$  and  $\rho_s$  are the tip and sample densities of states and  $T$  represents the barrier transmission probability for electrons of energy  $E$  at a given voltage  $V$ . Often the second term of Eq. (1) can be neglected. Then, under the conventional assumption of a monotonic variation of  $T$  with  $V$ ,  $dI/dV$  is a good measure of  $\rho_s$  at  $E=eV$  and exhibits the corresponding oscillations. This explains the better visibility of oscillations in  $dI/dV$  maps which we observe experimentally in agreement with previous results.<sup>3,4</sup>

The fact that  $dI/dV$  cannot directly be taken as the LDOS is evident from Fig. 1. At small  $V$  the constant current image closely follows the LDOS at the Fermi energy.<sup>5</sup> Figure 1 shows that the positions of the maxima in constant current images and in  $dI/dV$  data do not coincide (cf. dashed vertical lines). We therefore numerically evaluated Eq. (1) near a step in order to determine the constant current topograph ( $z$ ) and the  $dI/dV$  signal.

For clarity, we first consider a sinusoidal LDOS  $\rho_s \propto \sin(kx)$  where  $k$  is the wave vector and  $x$  is the lateral position [Figs. 2(a), 2(d)].  $k$  is linked to the energy of a surface-state electron via  $E-E_0 \propto k^2$ , where  $E_0$  is the surface-state band edge (cf. Fig. 4). The current  $I(x)$  is calculated as  $I(x) \propto \int_0^{eV} \rho_s(E, x)\rho_t T(E, eV, x) dE$  with a transmission factor

$$T(E, eV, x) = \exp\left[-z(x) \sqrt{\frac{4m}{\hbar^2} (\phi_t + \phi_s + eV - 2E)}\right]. \quad (2)$$

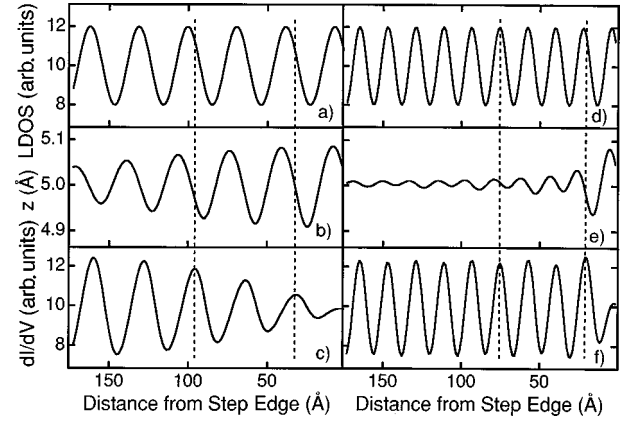


FIG. 2. Model calculations of the constant current images (b), (e) and  $dI/dV$  maps (c), (f) assuming sinusoidal densities of states  $\rho_s$ . (a), (d) display  $\rho_s$  at  $V$ . Calculations were performed for  $V=20$  mV (a)–(c) and  $V=200$  mV (d)–(f). The dashed vertical lines serve to guide the eye.

Here, the work functions of the W tip  $\phi_t$  and the Ag sample  $\phi_s$  are 4.55 and 4.74 eV, respectively;<sup>14</sup>  $m$  is the electron mass;  $\rho_t$  is assumed to be constant. To simulate the constant-current mode, at every position  $x$ ,  $z(x) = z_0 + \Delta z(x)$  ( $z_0 = 8$  Å) is adjusted to match the preset constant current value. Then,  $dI/dV$  is obtained from Eq. (1). At  $V=200$  mV [Figs. 2(d), 2(e), 2(f)],  $z$  and  $dI/dV$  exhibit the expected behavior. The  $z$  signal shows little oscillation because  $I$  is an integral over a wide range of energies and hence  $\rho_s$  oscillations with widely varying wavelengths. For positions not too close to the step,  $dI/dV$  closely resembles  $\rho_s$ . At  $V=20$  mV [Figs. 2(a), 2(b), 2(c)],  $z$  exhibits some oscillations with decaying amplitudes. The maxima positions show some similarity with those of  $\rho_s$  itself. The  $dI/dV$  signal strongly deviates from  $\rho_s$ . Both the amplitudes and the positions of the  $dI/dV$  maxima do not faithfully represent  $\rho_s$ . In particular, the relative displacement between the  $\rho_s$  maxima and the corresponding  $dI/dV$  maxima can be as large as  $\sim 6$  Å which corresponds to about one fifth of a wavelength. This affects the determination of scattering phases from  $dI/dV$  patterns. Moreover, the amplitude of the  $dI/dV$  oscillation is found to increase with the distance from the step.

The reason for these deviations can be determined from the numerical results. At low  $V$ ,  $I$  results from an integration over a narrow energy window. This causes a significant enhancement of the oscillation amplitude of  $z$  and hence influences the barrier transmission  $T$  which depends exponentially on  $z$  [Eq. (2)]. The wavelength  $\lambda_z$  of the  $z$  oscillation results from an integration over a small range of energies and differs slightly from the wavelength  $\lambda_\rho$  of the  $\rho_s$  oscillation at  $E=eV$ . For  $V>0$  ( $V<0$ ) we have  $\lambda_z \geq \lambda_\rho$  ( $\lambda_z \leq \lambda_\rho$ ). As a result there is a “beating” of  $dI/dV$  which is closely related to the product  $\rho_s T$ . [The second term in Eq. (1) is found to be negligible.]

A comparison of experimental  $dI/dV$  data for both positive and negative voltage [Figs. 3(a), 3(c)] with the calculated results based on a more realistic LDOS  $\rho_s$  [Figs. 3(b), 3(d)] shows good agreement. In this simulation, the variation of  $\rho_s$  was assumed to be described by an exponentially damped Bessel function  $1 - J_0$ .<sup>3,4</sup> Important observations are (i) the high amplitude of the second  $dI/dV$  maximum

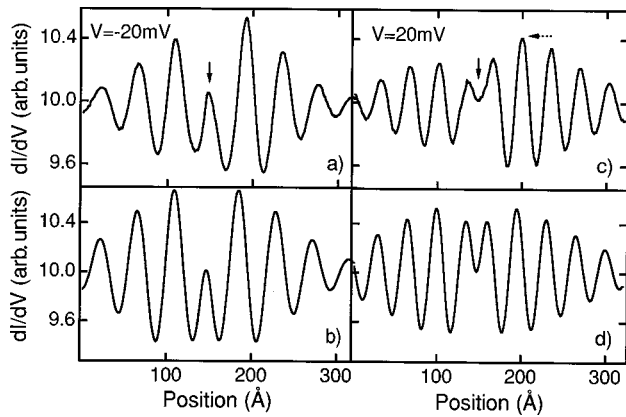


FIG. 3. Comparison of (a), (c) experimental  $dI/dV$  data obtained from a monatomic step and (b), (d) calculated results for  $V = -20$  mV and  $V = 20$  mV. Vertical arrows indicate the topographic step edge (defined as the position of steepest slope in the constant current image of Fig. 1(a)). The lower terrace is on the left hand side. The dashed arrow indicates the high amplitude of the second  $dI/dV$  maximum near the step edge.

[dashed arrow in Fig. 3(c)] from the step edge [vertical arrow in Fig. 3(c)], and (ii) the positive (negative) slopes of the  $dI/dV$  curves at the step edge for  $-20(+20)$  meV which are not caused by an increased maximum or oscillations of the LDOS  $\rho_s$ . Rather, both effects are due to the beating phenomenon described above. Moreover, for low tunneling voltages the envelope function of the  $dI/dV$  oscillations displays a convex shape (see Fig. 3) due to the predominant role of the beating. At higher tunneling voltages  $V_t > 50$  mV (not shown) it reflects the intrinsic exponential decay due to electron scattering. The difference in amplitudes<sup>3,4</sup> and phase of the standing wave pattern found experimentally on the lower and upper terraces [Figs. 3(a) and 3(c)] are not accounted for by the model.

From a series of similar comparisons of experimental and simulated  $dI/dV$  data over a range of voltages  $V$  (Fig. 4, solid circles) a dispersion curve  $E(k)$  (Fig. 4, solid line) is

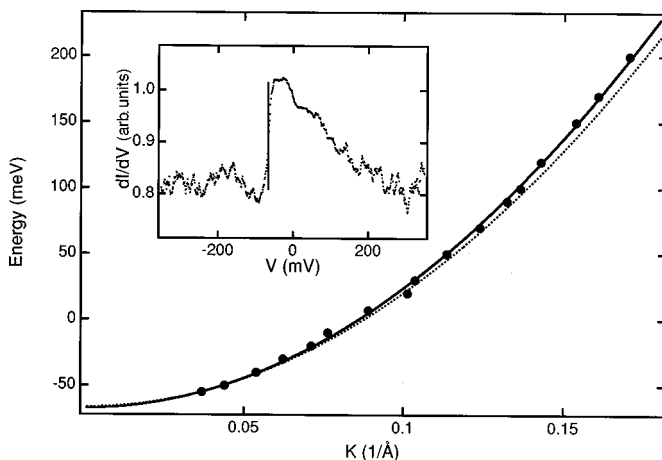


FIG. 4. Dispersion of the Ag(111) surface state. Solid circles:  $E(k)$  values (error  $\leq 3\%$ ) obtained from the  $dI/dV$  data using the modeling discussed in the text. Solid curve: Parabolic fit to these data. Dashed curve: Photoelectron spectroscopic data from Ref. 15; Inset:  $dI/dV$  spectrum taken on a clean  $1000 \text{ \AA}$  wide terrace on Ag(111).

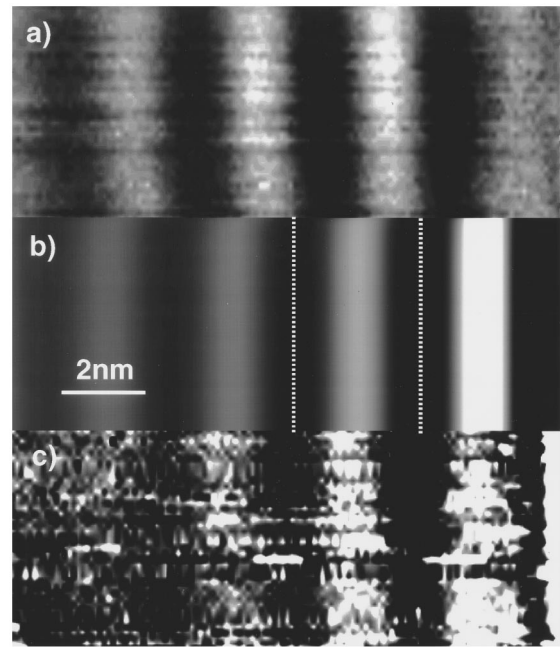


FIG. 5. Reconstruction of the local density of states.  $dI/dV$  map (a) taken at  $V = 20$  mV on the lower terrace near a monatomic step; the model LDOS near a step (b) agrees well with the recovered LDOS (c). The dashed vertical lines serve to guide the eye.

deduced from the STM data. The resulting band edge is  $E_0 = -67 \pm 3$  meV and the surface-state effective mass ratio is  $m^*/m = 0.42 \pm 0.02$ . The  $dI/dV$  spectrum, shown in the inset of Fig. 4 and taken with the tip over a clean  $1000 \text{ \AA}$  wide terrace, clearly confirms the onset of the surface state at  $-65 \pm 5$  meV. The good agreement between the present STM-derived dispersion and that derived from PES (Ref. 15) (Fig. 4, dashed curve) indicates that the STM tip does not cause perturbation of the Ag(111) surface state at the present level of precision.

Below, we propose a direct method to recover the underlying  $\rho_s$  of an uncorrugated surface which is illustrated in Figs. 5 and 6.<sup>16</sup> Since the integral in Eq. (1) is found to be

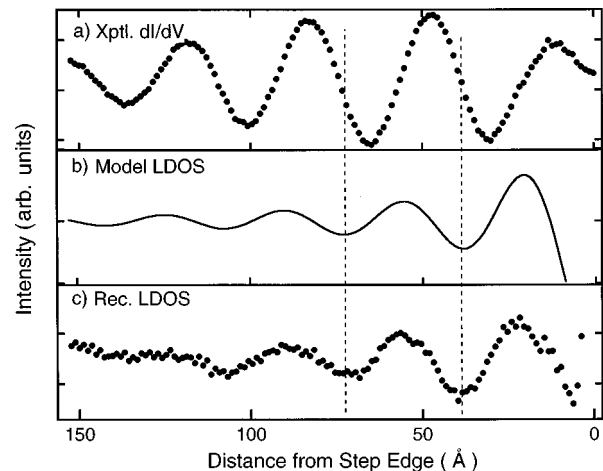


FIG. 6. Cross sections of the images shown in Fig. 5. (a)  $dI/dV$  map; (b) model LDOS near a monatomic step; the midpoint of the step edge is taken as the origin of the Bessel function; (c) recovered LDOS. The dashed vertical lines serve to guide the eye.

negligible in the voltage range of interest,<sup>10</sup> within our one-dimensional model,  $dI/dV$  is proportional to the product of  $\rho_s$  and the transmission factor  $T$ . The oscillation of the LDOS  $\rho_s$  at  $E = eV$  is now recovered from the  $dI/dV$  data by division with  $T$  [Figs. 5(c) and 6(c)]. For comparison  $\rho_s$  near a monatomic step on the Ag(111) surface is calculated using an exponentially damped Bessel function  $1 - J_0$  and the dispersion relation of Fig. 4 (solid line). As expected, the experimental  $dI/dV$  data shown in Figs. 5(a) and 6(a), differ in amplitude and phase from the model  $\rho_s$  [Figs. 5(b) and 6(b)]. The recovered  $\rho_s$  [Figs. 5(c) and 6(c)] closely corresponds to the model LDOS  $\rho_s$  [Figs. 5(b) and 6(b)] with respect to both, the positions of maxima and minima as well as the decaying oscillations away from the step edge. At distances closer than  $\sim 10$  Å from the step edge the surface may no longer be considered as flat and the STM-topograph no longer reflects electronic effects alone. Therefore, at these close distances, the reconstruction scheme presented above fails.

The essential quantity for reconstructing the oscillatory LDOS is the barrier transmission  $T$  which we evaluated using the WKB expression [Eq. (2)]. It is important to note that—in contrast to previous studies<sup>11</sup> which were mainly concerned with the energy dependency  $T(E)$ —our reconstruction relies on the distance dependency  $T(z)$ . Whereas  $T(E)$  may be difficult to determine<sup>11</sup>  $T(z)$  is described well by an exponential relation. The quantities of interest—the positions and relative amplitudes of the spatial LDOS oscillations—are not sensitive to a constant  $z$ -offset, whereas they are directly affected by the oscillating part of  $z$ . (We

note that the estimated  $z$  noise in our experiment of about 0.01 Å will cause a 2% variation in  $T$ .) Similarly, while a global variation of the work functions in Eq. (2) over the range of 3 to 6 eV does affect the absolute amplitudes of the spatial LDOS oscillations, there is little impact on their positions and relative amplitudes. We also verified by numerical simulations that over the bias voltage range studied here, the same is true for the small variation of  $T$  with the energy  $E$  and the momentum  $K$  parallel to the surface. Lateral variations of the tunneling barrier height that could in principle affect the reconstruction have not been observed in measurements of  $dI/dz$  on Ag(111) terraces, i.e.,  $dI/dz$  is featureless. To summarize, the main results of the reconstruction are robust with respect to reasonable changes of the parameters in Eq. (2).

In conclusion, we have discussed the interpretation of spectroscopic STM images ( $dI/dV$ ) in terms of the local density of states. We have shown that oscillations of the LDOS  $\rho_s$  can be derived from  $dI/dV$  maps at low tunneling voltages by a simultaneous measurement of high resolution topographic images. This finding may be of particular importance for the experimental determination of the underlying LDOS  $\rho_s$  when electron scattering at impurity sites, electrons confined within nanostructures at surfaces, or quasiparticles at superconductor surfaces are considered.

We thank K. Morgenstern for a critical reading of the manuscript. This work has been supported by the Swiss National Science Foundation.

<sup>1</sup>*Electronic Surface and Interface States on Metallic Systems*, edited by E. Bertel and M. Donath (World Scientific, Singapore, 1995), and references therein.

<sup>2</sup>S. Hüfner, *Photoelectron Spectroscopy* (Springer, Berlin, 1995).

<sup>3</sup>M. F. Crommie, C. P. Lutz, and D. M. Eigler, *Nature* (London) **363**, 524 (1993); **369**, 464 (1994).

<sup>4</sup>Y. Hasegawa and Ph. Avouris, *Phys. Rev. Lett.* **71**, 1071 (1993); Ph. Avouris and I.-W. Lyo, *Science* **264**, 942 (1994); Ph. Avouris, I.-W. Lyo, and R. E. Walkup, *J. Vac. Sci. Technol. B* **12**, 1447 (1994); Ph. Avouris, I.-W. Lyo, and P. Molinàs-Mata, *Chem. Phys. Lett.* **240**, 423 (1995).

<sup>5</sup>J. Tersoff and D. R. Hamann, *Phys. Rev. B* **31**, 805 (1985).

<sup>6</sup>H. F. Hess *et al.*, *Phys. Rev. Lett.* **62**, 214 (1989); H. F. Hess, *Physica C* **185-189**, 259 (1991).

<sup>7</sup>See, e.g., L. Bolotoff, H. Rauscher, and R. J. Behm, *Chem. Phys. Lett.* **234**, 445 (1995); J. A. Kubby and W. J. Greene, *J. Vac. Sci. Technol. A* **12**, 2009 (1994).

<sup>8</sup>J. A. Stroscio, R. M. Feenstra, and A. P. Fein, *J. Vac. Sci. Tech-*

*nol. A* **5**, 838 (1987); J. A. Stroscio, R. M. Feenstra, D. M. Newns, and A. P. Fein, *ibid.* **6**, 499 (1988); R. M. Feenstra, J. A. Stroscio, and A. P. Fein, *Surf. Sci.* **181**, 295 (1987).

<sup>9</sup>See, e.g., R. J. Hamers, *Annu. Rev. Phys. Chem.* **40**, 531 (1989); R. M. Feenstra, *Surf. Sci.* **299/300**, 965 (1994).

<sup>10</sup>G. Hörmandinger, *Phys. Rev. Lett.* **73**, 910 (1994); *Phys. Rev. B* **49**, 13 897 (1994).

<sup>11</sup>V. A. Ukraintsev, *Phys. Rev. B* **53**, 11 176 (1996).

<sup>12</sup>R. Gaisch *et al.*, *Ultramicroscopy* **42-44**, 1621 (1992).

<sup>13</sup>L. C. Davis, M. P. Everson, R. C. Jaklevic, and W. D. Shen, *Phys. Rev. B* **43**, 3821 (1991).

<sup>14</sup>H. B. Michaelson, *J. Appl. Phys.* **48**, 4729 (1977).

<sup>15</sup>R. Paniago, R. Matzdorf, G. Meister, and A. Goldmann, *Surf. Sci.* **336**, 113 (1995).

<sup>16</sup>Due to its different periodicity (as compared to the standing wave pattern) the topographic signal due to the atomic structure of the Ag(111) substrate does not cause a problem in reconstructing the LDOS.